First published in:

WISSENSCHAFTLICHE KONFERENZ "15 JAHRE FDIBA 2006"

RESEARCH AT ITM ON VEHICLE DYNAMICS

Jörg Wauer, Hartmut Hetzler, Carsten Proppe, Wolfgang Seemann, Christian Wetzel
Institut für Technische Mechanik, Universität Karlsruhe (TH), Germany
Bernhard Schweizer
Fachgebiet Mehrkörpersysteme, Universität Kassel, Germany

Abstract: *The actual Research at the Institut für Technische Mechanik on selected problems concerning vehicle dynamics is presented. Both the dynamics of automobiles and railcars is addressed. Our special focus is directed to friction-induced noise of automotive disk brakes including heat effects and the cross-wind stability of railcars.*

Key Words: *Railcars, Cross wind stability, Car disk brake, Friction-induced vibrations, Heat effects.*

Introduction

Dynamical problems in Automotive Engineering belong to the main traditional research areas of the Institut für Technische Mechanik at the Universität of Karlsruhe (TH). Significant work goes back to the late 80's when Wedig and Ammon (see [1,2], for instance) started the investigations to model uneven roads via a spectral power density approach. The activities were continued by research on wheel/rail contact dynamics of railway cars where Wauer was the main referee for the dissertation [3] of Morys. In 1997, an extended BMBF project on nonlinear dynamics was established [4], to which the Institut für Technische Mechanik contributed with examinations on friction-induced noise in disk brakes of cars (see [5,6], for instance). The contribution [6] was also the starting point to include heat effects in rotating structural members as rings or disks [7] but without final results until very recently. 2004 our current research work was started where problems on the dynamics of disk brake models including heat effects were taken up once more. Beyond this, the safety of railway cars under side wind excitation is a second important field in our research on vehicle dynamics. The progress in these two projects will be presented in this contribution.

1. Crosswind Stability of Railway Vehicles

The crosswind stability against overturning is a major design criterion for high speed railway vehicles. Recent developments in railway engineering have been showing a trend to faster, more energy efficient and more comfortable trains with a higher capacity of passenger transportation. These efforts are directly leading to light-weight cars with distributed traction. Unfortunately, these developments significantly alter the crosswind stability in a negative manner. Therefore, crosswind stability has become a crucial issue of modern railway vehicle design that cannot be solved easily as all counter-measures are very expensive. If a railway vehicle fails to be certified, ballasting is often the only possible solution. In recent years efforts have been made to derive an uniform rule in certifying railway vehicles. In this case especially probabilistic methods have been proposed [8], where crosswind stability is expressed as probability of failure, which can be computed by means of analytical or numerical approaches. In this case failure means the exceedance of a critical value of the so-called wheel unloading δQ .

1.1 Modeling of the system

The system consists of two parts: the multibody vehicle model and the environmental model. The environmental model itself has two components: the track and the aerodynamic model. A schematic sketch of the system is shown in Fig. 1. Commercial multi-body system software has been employed in order to accurately represent the vehicle, a cabin car. The elasticity of the carbody and the bogie frames has been neglected. On the other hand, nonlinearities of the spring and damper characteristics and the bump stops have been taken into account. The train is assum-

EVA-STAR (Elektronisches Volltextarchiv – Scientific Articles Repository)
http://digbib.ubka.uni-karlsruhe.de/volltexte/1000011211

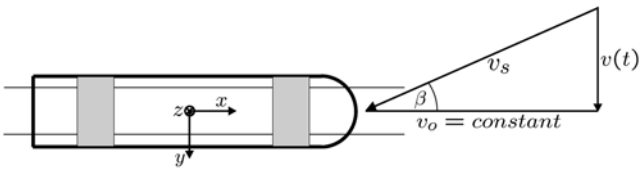

Figure 1. Coordinate system and wind velocity vector

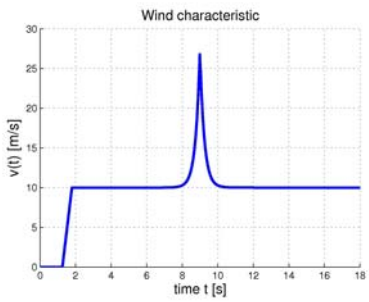

Figure 2. Representative gust shape

ed to move with constant velocity on a straight track.

Two wind scenarios are investigated:

- a train coming out of a tunnel immediately being hit by a gust;
- a train traveling on an embankment under constant mean wind load being hit by a gust.

The model for the crosswind consists of a superposition of the mean wind and the gust characteristic [9]. As the train speed is much higher than the velocity of the crosswind, the spatial correlation of the wind can be neglected. That means that the wind excitation is modeled in such a way, as if the train would be running through a frozen wind field. Hence the wind is designed as a function of the track variable s and must be transformed into the time domain as the computation has to be done in the time domain (see Fig. 2).

1.2 Simulation concept

For the calculation of the probability of failure P_f, it is necessary to evaluate the integral $P_f = \int_{\Omega_f} p_{Z*}(z^*)dz^*$ over the failure domain Ω_f, where z^* is the array of all stochastic variables of the system and $p_{Z*}(z^*)$ the joint probability density function. The failure domain Ω_f is the set of all arrangements of z^* which forces the wheel-unloading to fall below the safety margin. The integral can be simplified by using the law of conditional probability. The probability of failure is

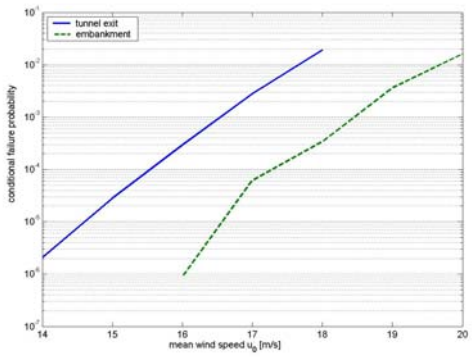

Figure 3. Comparison of failure probability for tunnel exit and embankment scenario (FORM results).

then obtained as $P_f = \int_{u_{0,d}}^{u_{0,t}} P(z \mid u_0) p(u_0) du_0$ where $P(z|u_0)$ is the failure probability conditioned to the mean wind speed u_0, $p(u_0)$ the pdf of u_0 and z the array z^* without u_0. In order to evaluate P_f, $P(z|u_0)$ and $p(u_0)$ have to be known. The latter can be obtained from meteorological measurements, while the former has to be computed.

The conditional failure probability $P(z|u_0)$ can be evaluated either by analytical methods, such as FORM or SORM or by numerical methods employing Monte Carlo simulation with variance reduction [10]. Here, all distributions are mapped to a standard Gaussian space, in which the shortest distance to the failure domain, the so called design point, is computed.

1.3 Results

Fig. 3 compares the conditional failure probability for the tunnel exit and the embankment scenario for a train speed of 160 km/h. As can be expected, failure probabilities for the embankment scenario are lower than for the tunnel exit. Stated in another way, the cabin car can sustain mean wind speeds that are approximately 2 m/s higher at the same failure level.

2. Automotive Disk-brake Vibrations

Disk-brakes of automobiles may exhibit a large variety of structural and acoustic vibrations, which are usually classified based on their frequency spectrum and the subjective impression to human observers. Our current research aims on understanding the instability mechanisms provoking the oscillations and the mechanisms sustaining them. In the latter context, the focus is set on self-excited low-frequency noises, usually referred to as “groan” and “muh”.

2.1 Experimental noise studies

Most measurement data on low-frequency vibrations are taken either on the car or on an entire brake assembly on a test rig. In both cases, the measurements are contaminated by the influence

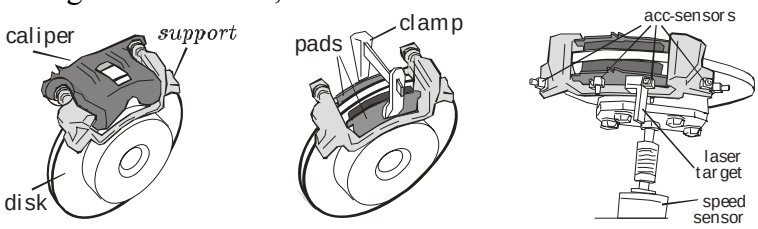

Figure 4. Experimental set up.

of diverse other parts (e.g. suspension, etc.) and the sensors have to be placed far away from the contact zone. Since the oscillations are supposed to be friction induced, the physical processes in this latter point may be of considerable importance. Hence, to allow for a clearer image, prior to measurement all dispensable parts had been removed and the calliper was replaced by a screw clamp. Surprisingly, the acoustic impression remained almost unchanged.

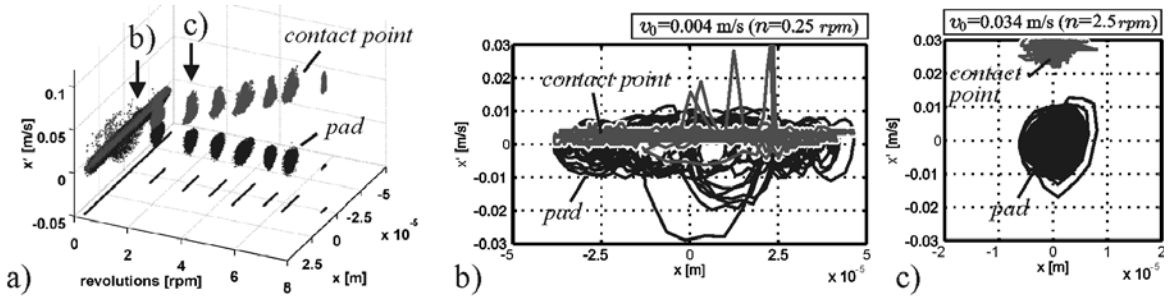

Figure 5. a) Phase plots (*x*-*x’*) of the pad and corresponding contact point speed for different speeds. b) Disk speed at 0.25 rpm. c) Disk speed at 2.5 rpm.

Fig. 5 shows phase diagrams (*x*-*x’*) of the pad’s motion for different driving speeds (black). Further, to each state (*x*-*x’*) the corresponding speed v_C of the contact point on the disk is dis-played (grey). The behaviour is threefold: while at very low speeds (Fig. 5b) the relative speed $v_{rel} = x' - v_C$ between pad and disc vanishes, this is not the case at higher speeds (Fig. 5c). At about 6.5 rpm vibrations cease totally. Hence, the common assumption of an underlying stick-slip mechanism does not seem to be a fully satisfying explanation. Further results and conclusions can be found in [11].

2.2 Analytical and numerical examination of friction-induced noise

The experimental results give rise to two questions: why does the static solution turn unstable and what mechanism sustains the self-excited vibrations? Since experiments showed that the coefficient of

sliding friction μ decays exponentially with relative speed, this classical mechanism – often referred to as *negative damping* - has been reinvestigated by means of nonlinear analysis.

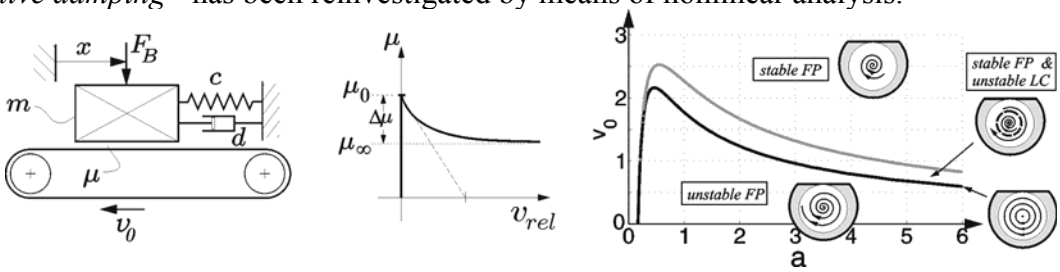

Figure 6. a) “Mass-on-a-conveyor”-model. b) Friction characteristic. c) Bifurcation behaviour.

To this end, the common “mass-on-a-conveyor”-minimal model was studied, incorporating a friction characteristic with exponential decay (Fig. 6). It was found out, that the static solution of stationary sliding may undergo a sub-critical Hopf-bifurcation [12].

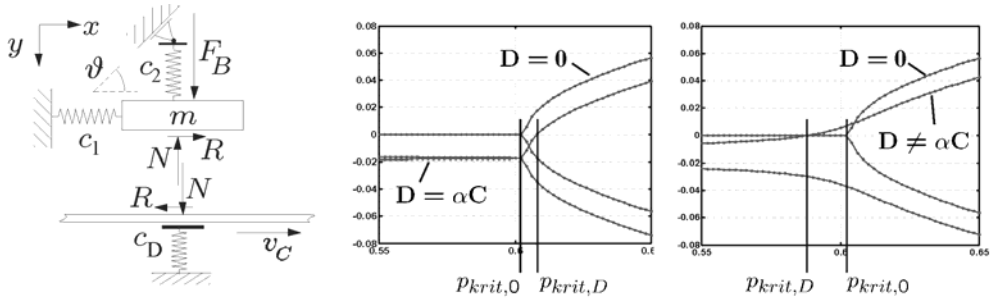

Figure 7. a) Minimal model to examine oscillatory instabilities due to friction.
b) Destabilization through damping.

Recent work on destabilizing phenomena concentrates on *eigenvalue coupling* leading to flutter-like oscillatory instabilities. As is well known, these so-called circulatory systems may be destabilized when damping is added – however, calculations in industrial applications still do not account for this effect. As a first result of our work, an easy-to-use criterion has been developed to test the effect of an arbitrary damping matrix on a given circulatory system (cf. Fig. 7).

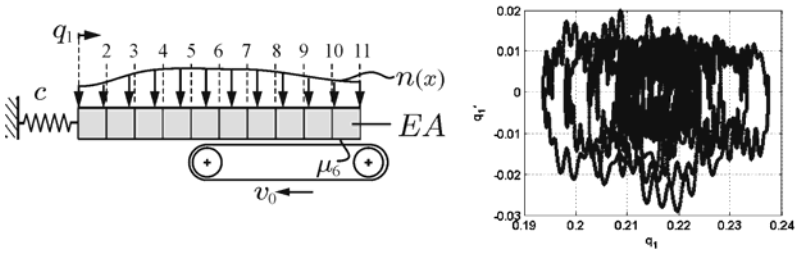

Figure 8. a) FE-discretized elastic beam, partially subjected to stick-slip friction.
b) Phase-plot of the left end’s displacement q_1 (node 1).

Besides destabilizing mechanisms, the effect of stick-slip friction on elastic structures is studied in order to clarify the experimental observations regarding limit-cycle behaviour at almost vanishing relative speeds. Since friction is a local property of the contact zone, a discretization by means of a FE-approach seems to be more appropriate than by global ansatz functions. It is found that especially at low driving speeds, the elastic properties may have considerable influence on the dynamics. Although the basic properties if stick-slip oscillators can still be observed (cf. Fig. 8) and therefore elastic properties are not very likely to cause the unexpected scaling behaviour of the pad’s phase diagrams with the relative speed (Fig. 5).

2.3 Heat effects

To discuss not only mechanical vibrations but to include heat effects, it is appropriate to model the rotating disk of the brake as a thermoelastic one and analyze the interacting displacements and the

temperature. To understand the basics, we actually consider in-plane vibrations $u(r,\varphi,t), v(r,\varphi,t)$ of a disk (see Fig. 9) rotating with constant angular speed Ω about the Z- axis of a stationary X,Y,Z reference frame together with the temperature $\vartheta(r,\varphi,t)$ above a reference value ϑ_0. There are body-fixed x,y,z coordinates where z and Z coincide and a body-fixed cylindrical e_r, e_φ, e_z reference frame in which basically, the field quantities are measured. The disk has inner and outer radii R_i and R_o, respectively and constant thickness h which is small so that a planar theory can be applied. As excitation, there is in general a simultaneous stationary force and heat source at that location where the pads are pushed against the disk.

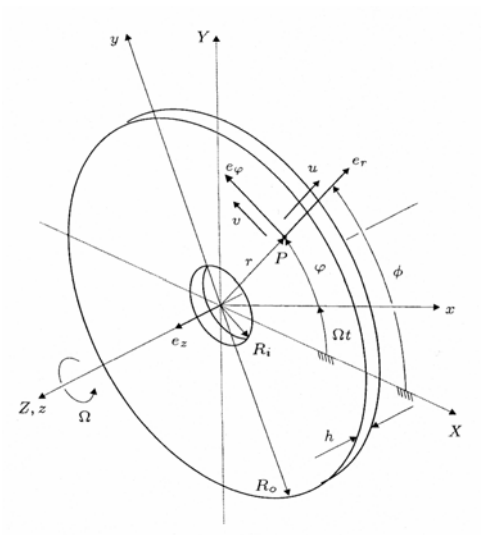

Figure 9. Rotating Disk.

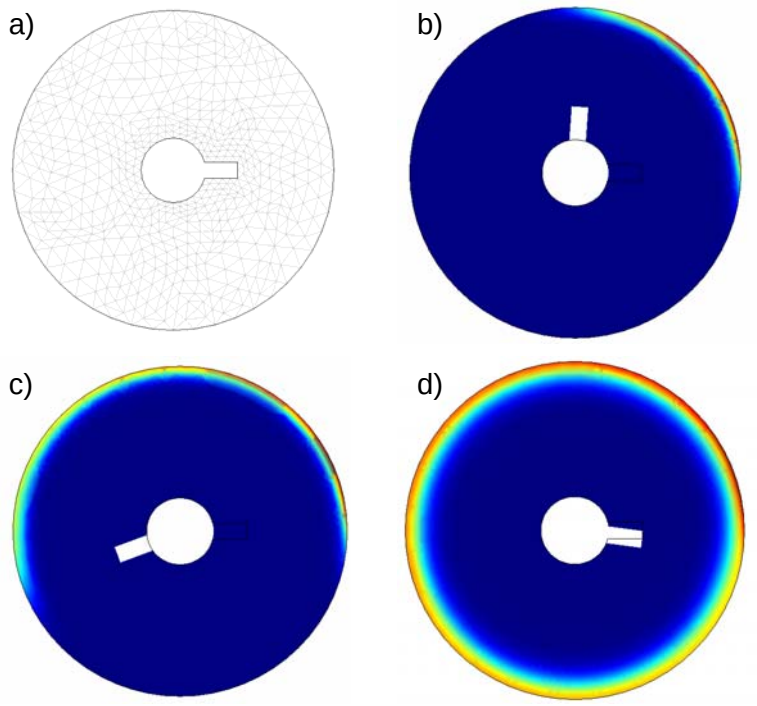

Figure 10. a) t=0sec; b) t=0.3sec; c) t=0.7sec; d) t=5sec

The governing equation for the coupled linear thermoelastic problem can be derived from the momentum, constitutive, energy, and entropy equations taking into account Fourier´s law of heat conduction [13]. Elimination of variables leads to the coupled mechanical and thermal field equations, which in body-fixed coordinates read as

$$\mu\nabla^2\underline{u} + (\lambda+\mu)\nabla(\nabla\cdot\underline{u}) + \rho\underline{k} = \rho(\ddot{\underline{u}} + 2\underline{\Omega}\times\dot{\underline{u}} - \Omega^2\underline{u}) + \alpha\nabla\vartheta, \quad \kappa\nabla^2\cdot\vartheta - c_v\dot{\vartheta} - \vartheta_0\alpha(\dot{\underline{\underline{\varepsilon}}}\cdot\cdot\underline{\underline{E}}) = -\rho r.$$

$\underline{u}$ denotes the displacement vector, μ and λ are the Lamé-constants, ρ is the density, $\underline{k}$ collects the volume forces, α is the coefficient of thermal expansion, κ denotes the coefficient of thermal conductivity, c_v is the heat capacity, $\underline{\underline{\varepsilon}}$ the linearized strain tensor, $\underline{\underline{E}}$ the unity tensor and r represents internal sources of heat. Problematic are the stationary source terms which in body-fixed coordinates become time-dependent. To avoid this explicit time-dependency, it is straightforward to translate the formulation into stationary coordinates by using the circum-ferential Eulerian coordinate $\phi = \varphi + \Omega t$. Based on the corresponding transformation, all problems of interest are dealt with.

Within this contribution, pure heat conduction only is evaluated. For the case that a heat source is acting at the stationary location $X = R_o, Y = 0$ and $Z = 0$, the transient behaviour of the temperature field $\vartheta(r,\varphi,t)$ for an annular disk with thermally insulated surfaces is shown in Fig. 13. The case of a really thermoelastic disk with both heat and force sources will be treated in a future paper.

References

1. Ammon, D., Wedig, W., *Identification of Power Spectra - Linear and Nonlinear Approaches*, in: Proc. ICOSSAR '89 *Structural Safety and Reliability*, 1989, San Francisco, Paper No. T23D-05.
2. Ammon, D., *Simulation von Fahrbahnunebenheiten -- Theorie, Modelle und Verifikation*, in: VDI-Tagung *Berechnung im Automobilbau*, 1990, Würzburg, VDI Ber. Nr. 816, VDI-Verlag, Düsseldorf, 1990, 589-598.
3. Morys, G.B., Zur Entstehung und Verstärkung von Unrundheiten an Eisenbahnrädern bei hohen Geschwindigkeiten, Diss. Universität Karlsruhe (TH), 1998.
4. Popp, K. (Ed.), Detection, Utilization and Avoidance of Nonlinear Dynamical Effects in Engineering Applications, Shaker, Aachen, 2001.
5. Schmalfuß, C., Theoretische und experimentelle Untersuchungen von Scheibenbremsen, Fortschr.-Ber. VDI, Reihe 12, Nr. 494, VDI-Verlag, Düsseldorf, 2002.
6. Heilig, J., Instabilitäten in Scheibenbremsen durch dynamischen Reibkontakt, Fortschr.-Ber. VDI, Reihe 12, Nr. 515, VDI-Verlag, Düsseldorf, 2002.
7. Wauer, J., Heilig, J., *Thermoelastic Vibrations of Rotating Cylindrical Structures Generated by a Space-fixed Heat Source,* in: Proc. ISROMAC-9, Y. Tsujimoto (Ed.), DD-ABS-008, Honolulu, USA, 2002.
8. Carrarini, A., Reliability based analysis of the crosswind stability of railway vehicle Diss. TU Berlin, 1998.
9. Delaunay, D., Locatelly, J.P., *A gust model for the design of large horizontal axis wind turbines: completion and validation,* in: Proc. European Comm. Wind Energy Conf., Madrid, Spain, 1990, 176-180.
10. Proppe C., Pradlwarter H.J., Schuëller G.I., Equivalent linearization and Monte Carlo simulation in stochastic dynamics, *Probabilistic Engineering Mechanics* **18**, 2003, 1-15.
11. Hetzler H., Seemann W., Schwarzer D., *Analytical investigations of Hopf-bifurcations occuring in a 1-DOF sliding-friction oscillator with application to disc-brake vibrations*, in: Proc. ASME Design Eng. Techn. Conf. (IDETC), Long Beach, USA, 2005.
12. Hetzler H, Seemann J, *Friction Induced Brake Vibrations At Low Speeds – Experiments, State-Space Reconstruction And Implications On Modelling,* in: Proc. ASME Int. Mech. Eng. Congress & Exhib. (IMECE), Chicago, USA, 2006.
13. Altenbach, J., Altenbach, H., *Einführung in die Kontinuumsmechanik,* Teubner, Stuttgart, 1994.

Prof. Dr.-Ing. Dr. h. c. Jörg Wauer
Universität Karlsruhe (TH)
Institut für Technische Mechanik
Kaiserstr. 12, Postfach 6980
76128 Karlsruhe, Deutschland
Tel.: 0049 / 721 / 608 26 60
Fax: 0049 / 721 / 608 60 70
E-Mail: wauer@itm.uni-karlsruhe.de